ACS APPLIED MATERIALS & INTERFACES

Research Article

www.acsami.org

Marine Biofouling Resistance of Polyurethane with Biodegradation and Hydrolyzation

Wentao Xu,[†] Chunfeng Ma,*[,†] Jielin Ma,[†] Tiansheng Gan,[†] and Guangzhao Zhang*[,†,‡]

[†]Faculty of Materials Science and Engineering, South China University of Technology, Guangzhou 510640, People's Republic of China

[‡]Hefei National Laboratory for Physical Sciences at Microscale, Department of Chemical Physics, University of Science and Technology of China, Hefei 230026, People's Republic of China

Supporting Information

ABSTRACT: We have prepared polyurethane with poly(ε-caprolactone) (PCL) as the segments of the main chain and poly(triisopropylsilyl acrylate) (PTIPSA) as the side chains by a combination of radical polymerization and a condensation reaction. Quartz crystal microbalance with dissipation studies show that polyurethane can degrade in the presence of enzyme and the degradation rate decreases with the PTIPSA content. Our studies also demonstrate that polyurethane is able to hydrolyze in artificial seawater and the hydrolysis rate increases as the PTIPSA content increases. Moreover, hydrolysis leads to a hydrophilic surface that is favorable to reduction of the frictional drag under dynamic conditions. Marine field tests reveal that polyurethane has good antifouling ability because polyurethane with a biodegradable PCL main chain and hydrolyzable PTIPSA side chains can form a self-renewal surface. Polyurethane was also used to carry and release a relatively environmentally friendly antifoulant, and the combined system exhibits a much higher antifouling performance even in a static marine environment.

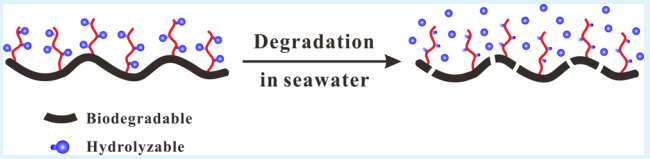

KEYWORDS: *polyurethane, poly(ε-caprolactone), poly(triisopropylsilyl acrylate), hydrolysis, degradation, antibiofouling*

INTRODUCTION

It is well-known that marine biofouling is a worldwide problem for maritime and aquatic industries.[1−3] It increases the hydrodynamic drag of ships, accelerates the corrosion of a metallic substrate, blocks the cooling cycle pipe, decreases the service life of marine equipment, and affects aquaculture systems. Biocidal coatings containing heavy metals are effective for combating marine fouling, but they are under environmental scrutiny because they are detrimental to nontarget organisms and ecologically harmful.[4,5] It is urgent to develop environmentally friendly systems for antibiofouling. For this purpose, poly(dimethylsiloxane) elastomers,[6,7] amphiphilic nanostructured coating,[8−12] zwitterionic polymers,[13,14] and self-generated hydrogel[15,16] have been prepared in recent years. Yet, their antibiofouling ability in a marine environment needs improvement.

Hydrolyzable polymers have been used for antibiofouling because their hydrolysis and dissolution can lead to a self-polishing surface and the release of incorporated biocides.[17,18] Silyl acrylate based polymers are typical hydrolyzable polymers with stable hydrolysis rates and self-smoothing properties. Moreover, their hydrolysis also positively contributes to the hydrodynamics of the ship's hull by reducing frictional drag and the total amount of fuel consumed. However, the self-polishing of silyl acrylate based polymers with hydrolyzable side chains mainly depends on the content of pendant silyl ester groups and the seawater motion. They generally exhibit poor mechanical properties and antibiofouling ability, especially in a static marine environment.[1,17,19−21] It is important to optimize the structure of a silyl acrylate copolymer to improve its antibiofouling ability under static conditions. Bressy et al. reported that poly(methyl methacrylate-*b*-*tert*-butyldimethylsilyl methacrylate) diblock copolymers have better control of the self-polishing rate compared to random copolymers.[22] The marine coatings based on the diblock copolymers exhibited good antifouling ability in the Mediterranean Sea for 18 months.[23]

Recently, we have developed marine antibiofouling materials based on degradable polyurethane with ε-caprolactone and glycolide (GA) copolyester oligomer as the segments of the main chain. The degradation of polyurethane in a marine environment leads to a self-renewal surface that can stop the settlement of marine biofouling even in a static marine environment.[24] However, the self-polishing rate is only modulated by the GA content. This limits its application because a high GA content would give rise to low adhesion strength and poor mechanical stability. Actually, it is a contradiction to improve the degradation rate and mechanical properties of degradable polymers. Here, we present a novel polyurethane with poly(ε-caprolactone) (PCL) segments in the main chain and poly(triisopropylsilyl acrylate) (PTIPSA) side chains, where the former are able to degrade in a marine environment because of the attack of seawater and microorganisms, whereas the latter have been commercially used in a

Received: November 29, 2013
Accepted: February 28, 2014
Published: February 28, 2014

   dx.doi.org/10.1021/am4054578 | ACS Appl. Mater. Interfaces 2014, 6, 4017−4024

Scheme 1. Synthesis of Degradable Polyurethane with Hydrolyzable Side Chains

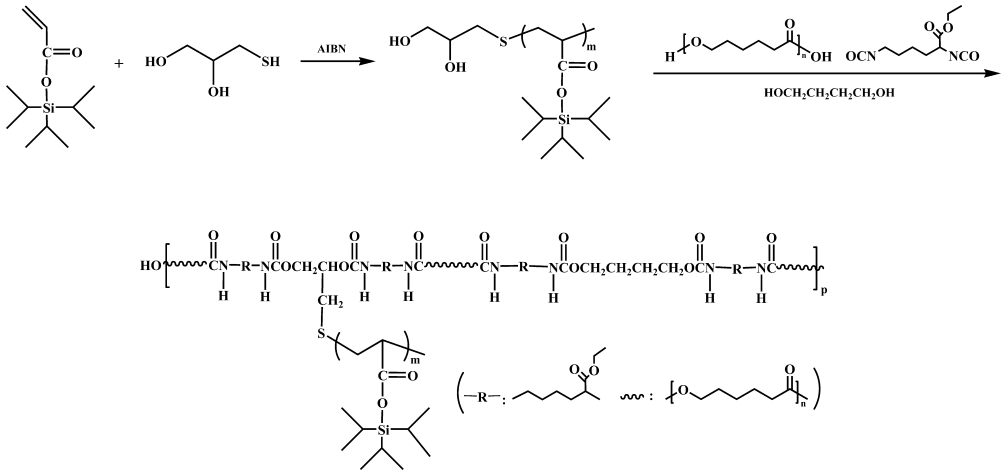

Table 1. Characterization Data of PU-S*x*

sample	LDI/PCL/PTIPSA(OH)$_2$/1,4-BD[a]	PTIPSA content (wt %)[b]	M_n[c] (g/mol)	M_w/M_n[c]	T_g (°C)[d]	T_m (°C)[d] [ΔH_m(J/g)]	$T_{50\%}$ (°C)[e]
PU-S0	6.6/1/0/5.6	0	15000	1.6	−51.7	33.5 [1.07]	326
PU-S7	6.6/1/0.25/5.35	7.3	10000	1.4	−52.3	33.0 [0.12]	334
PU-S14	6.6/1/0.5/5.1	13.8	12000	1.3	−52.6		341
PU-S22	6.6/1/0.93/4.67	22.3	13000	1.5	−53.9		346
PU-S32	6.6/1/1.48/4.12	32.4	11000	1.3	−55.8, −20.9		351
PU-S40	6.6/1/2.22/3.38	40.1	12000	1.3	−57.9, −22.6		392

[a]Feed molar ratio. [b]Determined by ^{1}H NMR. [c]Determined by GPC. [d]Determined by DSC. [e]Temperature at 50% weight loss as determined by TGA.

self-polishing coating under a sailing state. The self-polishing rate of the surface constructed by polyurethane determined by degradation and hydrolysis can be regulated by varying its composition. Moreover, the introduction of biodegradable PCL into the silyl acrylate polymers can also improve dissolution of the hydrolytic moieties without the help of shear force, which facilitates antibiofouling in the static state. We have investigated the degradation, hydrolysis, and antifouling property of polyurethane. Our aim is to develop antibiofouling materials in both static and dynamic marine environments.

EXPERIMENTAL METHODS

Materials. Poly(ε-caprolactone) diol (PCL; M_w = 2000 g/mol) was from Perstorp. Triisopropylsilyl acrylate (TIPSA) was synthesized following a procedure elsewhere.[25,26] 3-Mercapto-1,2-propanediol (TG), 1,4-butanediol (1,4-BD), and dibutyltin dilaurate were from Aldrich. L-Lysine ethyl ester diisocyanate (LDI) was from Dahong Chemical and was used as received. 2,2-Azobis(isobutyronitrile) (AIBN) was recrystallized twice from methanol. TIPSA was distilled under reduced pressure before use. PCL was dried under reduced pressure for 2 h prior to use. Tetrahydrofuran (THF) was refluxed over CaH_2 and distilled prior to use. Lipase PS purchased from Aldrich was purified by filtration and freeze-drying before use. 4,5-Dichloro-2-octyl-isothiazolone (DCOIT) was kindly presented by Fangfu Chemical Co. (Guangzhou). Artificial seawater (ASW) was prepared according to ASTM D1141-98 (2003). Other reagents were used as received. The synthesis of degradable polyurethane with hydrolyzable side chains is illustrated in Scheme 1.

Synthesis of PTIPSA(OH)$_2$. By the introduction of dihydroxyl at one end and control of the molecular weight, PTIPSA(OH)$_2$ was prepared by radical telomerization with TG as a chain-transfer reagent.[27,28] Typically, TIPSA (6.384 g, 28 mmol), AIBN (0.0032 g, 0.05 wt % based on monomers), TG (0.432 g, 4 mmol), and THF (15 mL) were introduced into a 100 mL three-necked flask under a nitrogen purge, and polymerization was carried out at 70 °C for 12 h. The product was precipitated into methanol, isolated, and dried under vacuum (yield: 70.0%). ^{1}H NMR (400 MHz, $CDCl_3$, ppm): 3.80 ($HOCH_2CH(OH)$), 3.55−3.67 ($HOCH_2CH(OH)$), 2.78 ($CH(OH)$-CH_2S), 2.54 (CH_2CHCOO), 1.74 (CH_2CHCOO), 1.27 ($SiCH(CH_3)_2$), 1.05 ($SiCH(CH_3)_2$). IR: 3450 (OH), 2950 (CH_3), 1730 (C═O), 883 (Si−C) cm^{-1}. M_n and PDI of PTIPSA(OH)$_2$ determined by gel permeation chromatography (GPC) are 1400 g/mol and 1.25, respectively.

Synthesis of Polyurethane with PTIPSA Side Chains. Polyurethane with PTIPSA side chains was synthesized via a condensation reaction in THF under a nitrogen atmosphere.[29−31] LDI was reacted with PCL at 80 °C for 1 h, yielding a prepolymer. Subsequently, PTIPSA(OH)$_2$ was introduced, and the reaction was conducted at 80 °C for another 1 h. Finally, 1,4-BD and DBT were added as the chain extender and catalyst, respectively, and the mixture was allowed to react at 90 °C for 3 h. The reaction was monitored by Fourier transform infrared spectroscopy (FTIR; Figure S1 in the Supporting Information, SI). The resulting polymer was precipitated in excess hexane under stirring and allowed to stand overnight. Then, the precipitate was filtered, washed three times with a little hexane, and vacuum-dried for 24 h. The yield for polyurethane was above 90%. ^{1}H NMR (400 MHz, $CDCl_3$, ppm): 4.20 ($CHCOOCH_2CH_3$), 4.30 ($CHCOOCH_2CH_3$), 1.27 ($CHCOOCH_2CH_3$), 3.15 ($NCH_2CH_2CH_2CH_2$), 1.80 ($NCH_2CH_2CH_2CH_2$), 1.64 ($NCH_2CH_2CH_2CH_2$), 1.50 ($NCH_2CH_2CH_2CH_2$), 4.05 ($COCH_2CH_2CH_2CH_2CH_2O$), 2.3 ($COCH_2CH_2CH_2CH_2CH_2O$), 1.64 ($COCH_2CH_2CH_2CH_2CH_2O$), 1.38 ($COCH_2CH_2CH_2CH_2CH_2O$), 3.87 ($OCH_2CH_2CH_2CH_2O$), 1.52 ($OCH_2CH_2CH_2CH_2O$), 1.27 ($SiCH(CH_3)_2$), 1.05 ($SiCH(CH_3)_2$). IR: 3360 (NH), 2950 (CH_3), 2860 (CH_2), 1730 (C═O), 883 (Si−C) cm^{-1}. For convenience, polyurethane with PTIPSA side chains is designed as PU-S*x*, where *x* is the weight percentage of PTIPSA estimated by ^{1}H NMR. The characterization data are summarized in Table 1, and the details can be found in the SI.

Characterization. *^{1}H NMR Spectroscopy.* ^{1}H NMR spectra were recorded on a Bruker AV400 NMR spectrometer using $CDCl_3$ as the solvent and tetramethylsilane as the internal standard.

FTIR. FTIR spectra were recorded over 64 scans with a resolution of 4 cm^{-1} on a Bruker VECTOR-22 IR spectrometer. The samples were prepared by a KBr disk method.

GPC. The number- and weight-average molecular weights (M_n and M_w) and polydispersity index (PDI; M_w/M_n) were determined by GPC at 35 °C on a Waters 1515 chromatograph using a series of monodisperse polystyrenes as the standard and THF as the fluent with a flow rate of 1.0 mL/min.

Thermal Analysis. Differential scanning calorimetry (DSC) was performed on a Netzsch DSC 204F1 differential scanning calorimeter under a nitrogen flow of 50 mL/min. Samples were quickly heated to 100 °C, kept for 5 min to remove thermal history, then cooled to −80 °C at a rate of 10 °C/min, and finally reheated to 100 °C at the same rate. All DSC traces were from the second heat to minimize the effects of thermal history. The glass transition temperature (T_g) was taken as the midpoint of the transition. Clearly, T_g decreases with the PTIPSA content because the PTIPSA side chains can restrict the compatibility of the hard and soft segments of polyurethane (Table 1). The melting temperature (T_m) was taken as that corresponding to the maximum heat flow in the reheating process. The melting enthalpy change (ΔH_m) related to crystallization of the PCL phases was assessed by integration of the area of the melting peak. T_m and ΔH_m decreases as the PTIPSA content increases (Table 1), indicating that the introduction of PTIPSA side chains weakens crystallization of the PCL segments (Figure S7 in the SI).

Thermogravimetric analysis (TGA) was performed on a Netzsch TG 209F1 instrument under a nitrogen atmosphere at a heating rate of 10 °C/min in the range of 25−800 °C. PU-S*x* exhibits a new decomposition at high temperature (380−400 °C) in comparison with PU-S0 (Figure S8 in the SI). Moreover, the decomposition temperature ($T_{50\%}$) increases with the PTIPSA content (Table 1). Accordingly, the presence of PTIPSA side chains improves the thermal stability of polyurethane.

Enzymatic Degradation. Enzymatic degradation was monitored by using a quartz crystal microbalance with dissipation (QCM-D) and surface plasmon resonance (SPR). The polyurethane films were prepared by spin casting of the PU-S*x* solution in a THF solution (5 mg/mL) on a spin coater (CHEMAT, KW-4) at 4000 rpm in air. QCM-D and the AT-cut quartz crystal with a fundamental resonant frequency of 5 MHz were from Q-sense AB (Sweden). The details about the QCM-D can be found elsewhere.[32,33] Briefly, the QCM-D simultaneously monitors changes in the resonance frequency (Δf) and dissipation (ΔD) in real time. Δf is related to the change in the mass attached to the oscillating sensor surface, whereas ΔD is related to the viscoelasticity of the adsorbed layer. For a rigid film in vacuum or air, if it is evenly distributed and much thinner than the crystal, Δf is related to Δm and the overtone number (n = 1, 3, 5, ...) by the Sauerbrey equation[32]

$$\Delta m = -\frac{\rho_q l_q}{f_0}\frac{\Delta f}{n} = -C\frac{\Delta f}{n} \quad (1)$$

where f_0 is the fundamental frequency, ρ_q and l_q are the specific density and thickness of the quartz crystal, respectively, and C is the constant of the crystal (17.7 ng/cm^2·Hz). In the present study, ASW was used as the reference and the lipase PS solution (0.5 mg/mL) was delivered to the surface at a flow rate of 150 μL/min. The changes in the frequency (Δf) and dissipation (ΔD) give information about the degradation and structural change of the polyurethane films. All of the experiments were performed at 25 °C, and the presented data were from the third overtone (n = 3). The relative standard deviations for Δf and ΔD were less than 4.0%.

SPR measurements were performed on a SPR Navi 210A (Bionavis) instrument equipped with an autosampler accessory at 25 °C. The amount of mass change on the gold sensor slide can be followed by monitoring the change in the angular position (angular scan mode) over time.[34,35] The SPR angle shift is linear to the added mass of the layer with 0.1° ≈ 1 ng/mm^2. The Lipase PS solution (0.5 mg/mL) was delivered to the surface at a flow rate of 50 μL/min. The relative standard deviation for the angle shift was less than 5%.

Hydrolytic Degradation. The hydrolytic degradation testing was conducted in ASW at 25 °C. The PU-S*x* film on an epoxy resin panel (20 × 20 mm in size) was prepared via a solution-casting method, as reported before.[24] The weighted sample of each dried coating together with its panel was incubated in a tank of ASW that was changed every 2 weeks. At predetermined time points, the sample was taken out, rinsed three times with deionized water, and then dried at 25 °C until a constant weight. The mass loss (wt %) was estimated with the equation

$$\text{mass loss (wt \%)} = \frac{w_0 - w_t}{w_0 - w_{panel}} \times 100 \quad (2)$$

where w_0, w_t, and w_{panel} are the initial weight of the panel coated with PU-S*x*, the weight of the coated panel at time t, and the weight of the panel without coating, respectively. With the area of the epoxy resin panel fixed and the same solid content and volume of the PU-S*x* solution, each film has a weight of ∼116 ± 2 mg. The self-polishing rate is defined as the mass loss (wt %) per day. For each sample, three coated panels were prepared and measured, and each data point was averaged over three successive and consistent measurements.

Contact Angle (CA) Measurement and Attenuated Total Reflectance Fourier Transform Infrared Spectroscopy (ATR-FTIR). The stationary CA measurement was conducted on a Contact Angle System OCA40 (Dataphysics) at 25 °C by depositing a water drop of 3 μL on the PU-S*x* surface. Five different points on each sample were tested to obtain an average value. The IR spectra were recorded using a Bruker Vertex 70 FTIR spectrometer in ATR mode in the 600−4000 cm^{-1} range at room temperature with a resolution of 4 cm^{-1} and an accumulation of 32 scans. The samples were removed from ASW at different time intervals, rinsed three times using deionized water, and dried at 25 °C before the CA and ATR-FTIR measurements.

Scanning Electron Microscopy (SEM). The surface morphology of the PU-S*x* film after immersion in ASW as a function of time was observed by a Quanta 200 scanning electron microscope (Philips-FEI Corp., The Netherlands) operating at 15 kV. All of the samples were sputter-coated with gold to minimize sample charging.

Marine Field Test. The field test was performed at the inner Xiamen bay (24°45′N, 118°07′E) in China following GB 5370-2007. In brief, the samples applied to the epoxy resin panels (300 × 80 × 3 mm^3) were lowered into seawater at depths of 0.2−2.0 m from a stationary experimental raft starting on May 07, 2013. After a certain period of time, the panels were taken out of the sea, carefully washed with seawater, and photographed, and then they were immediately placed back into the seawater to continue the test. Panels coated with polyurethane containing different PTIPSA contents were tested. The molecular weight (M_n) of PU-S*x* varied from 10000 to 15000 g/mol. Variation of the molecular weight of the samples was attributed to their difference in the side-chain content and large polydispersity.[29] The panels coated with PU-S40 and poly(methyl methacrylate-*co*-triisopropylsilyl acrylate) (PMS42) in combination with DCOIT (∼10 wt %) were also examined to evaluate the antifoulant release. PMS42 (M_n = 1.5 × 10^4 g/mol; PDI = 1.6) with 42.3 wt % of PTIPSA was prepared by conventional radical polymerization following a procedure reported elsewhere.[22]

RESULTS AND DISCUSSION

Because the structure of PU-S*x* contains a polyester main chain, it is expected to degrade upon the enzymatic attack of microorganisms present in the seawater.[36,37] We first examined enzymatic degradation by use of QCM-D. Figure 1 shows the time dependence of the frequency shift (Δf) and energy dissipation shift (ΔD) for enzymatic degradation of polyurethane with different PTIPSA contents in ASW. For PU-S0, after lipase PS is introduced, Δf increases and gradually levels off. Actually, we can also observe a small decrease in Δf before

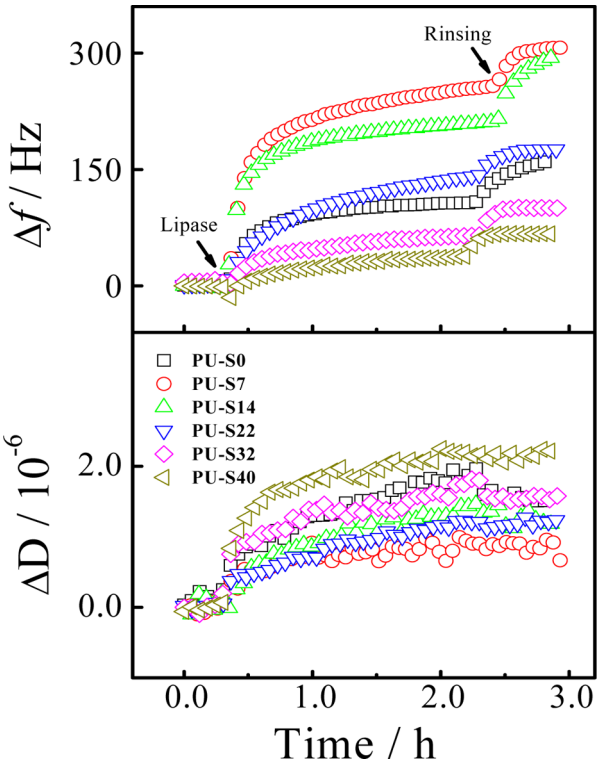

Figure 1. Time dependence of the frequency shift (Δf) and dissipation shift (ΔD) for enzymatic degradation of polyurethanes with different PTIPSA contents in ASW at 25 °C.

the increase in a short time scale of 0.5 h (not shown), indicating the adsorption of lipase on the film. It is not significant in a large time scale because it is too small relative to the increase of Δf. After rinsing with seawater, Δf exhibits a marked increase relative to the baseline. It is known that the increase of mass on the sensor surface causes the frequency to decrease.[38,39] The increase in Δf indicates a mass loss of the polyurethane film, or the polyurethane film degrades into small molecules that disperse into the solution. For PU-S*x* with a PTIPSA content of less than 22 wt %, a faster degradation can be observed, reflected in the bigger increase in Δf than that for PU-S0. Note that the PCL content in PU-S*x* only changes from 56.4 to 51.6 wt % (Figure S4 in the SI). The faster degradation arises from PTIPSA side chains that destroy the regularity of PCL segments and hinder their crystallization[40] (see Figure S7 in the SI). Further increasing the PTIPSA content leads Δf to be much smaller (for PU-S32 and PU-S40); that is, the degraded mass becomes lower because the PCL content decreases. Another reason is that PTIPSA side chains at higher content tend to migrate to the polyurethane surface because of their low surface energy and form a PTIPSA-rich surface, which prevents PCL segments from enzymatic attack.[41] On the other hand, it is well-known that ΔD increases with the thickness but decreases with the rigidness of the layer. Namely, a dense and rigid structure leads to a small dissipation of energy, whereas a looser structure results in a larger dissipation.[33,38] For all of the PU-S*x* films, ΔD increases with time, indicating that enzymatic degradation leads to a surface with a nonuniform structure. In the case of PU-S0 with higher crystallinity, the enzyme first attacks the amorphous region and then the crystalline area, and the former is faster than the latter, leading to a porous structure.[38] For polyurethane with a PTIPSA content, the difference of amorphous and crystalline area in the degradation rate becomes smaller as the crystallinity decreases. However, PTIPSA side chains and the undegraded PCL form a nonuniform structure after some PCL segments degrade, leading ΔD to increase, and the surface rigidity decreases. Moreover, ΔD increases with the film thickness.[42] As the PTIPSA content increases, the enzymatic degradation decreases, leaving a thicker film. Consequently, ΔD increases with the PTIPSA content. Anyhow, the surface constructed by polyurethane with PTIPSA side chains can be decomposed and eroded under enzymatic attack in a marine environment.

Enzymatic degradation was also examined by SPR (Figure 2). After a lipase PS solution is introduced, the SPR angle shows a

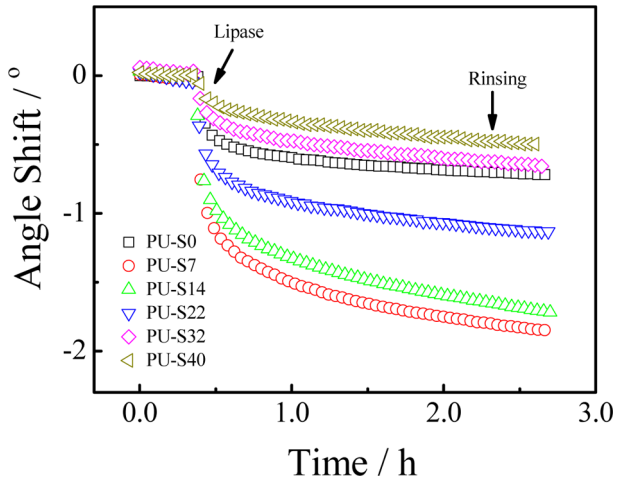

Figure 2. Time dependence of the SPR angle shift for enzymatic degradation of polyurethanes with different PTIPSA contents in ASW at 25 °C.

sharp decrease and gradually levels off, indicating mass loss of the films. For PU-S0, the decrease in the SPR angle after rinsing is ~0.73°. For PU-S7 and PU-S14 with a PTIPSA content of less than 22 wt %, larger angle shifts can be observed because polyurethane has a lower crystallinity and degradation is enhanced. Further increasing the PTIPSA content (for PU-S32 and PU-S40) leads the angle shift to decrease in that degradation decreases because of a decrease of the PCL content or surface passivation induced by migration of the PTIPSA side chains.[41] This is consistent with the QCM-D results.

The mass loss of the PU-S*x* samples can be estimated by the SPR shift. For PU-S0, PU-S7, PU-S14, PU-S22, PU-S32, and PU-S40, the mass loss values are 7.3, 18.5, 17.1, 11.4, 6.5, and 5.0 ng/mm^2, respectively. We can also estimate the mass loss via the frequency shift measured by QCM-D in terms of the Sauerbrey equation. For PU-S0, PU-S7, PU-S14, PU-S22, PU-S32, and PU-S40, they are 9.5, 18.0, 17.4, 10.3, 6.0, and 4.0 ng/mm^2, respectively. Clearly, the mass loss obtained by SPR is close to that from QCM-D except that of PU-S0. It is known that the mass estimated from the Sauerbrey equation is a hydrodynamic mass that includes those of polymer and coupled water,[33] whereas that estimated from the SPR shift is the mass of the polymer. PU-S*x*, except PU-S0, is hydrophobic and the coupled water is very limited, so that the mass loss estimated from SPR is close to that from QCM-D. PU-S0 is more hydrophilic and can couple more water molecules, which makes a bigger difference between them.

dx.doi.org/10.1021/am4054578 | ACS Appl. Mater. Interfaces 2014, 6, 4017−4024

Figure 3 shows the time dependence of the mass loss of polyurethane with different PTIPSA contents in ASW at 25 °C.

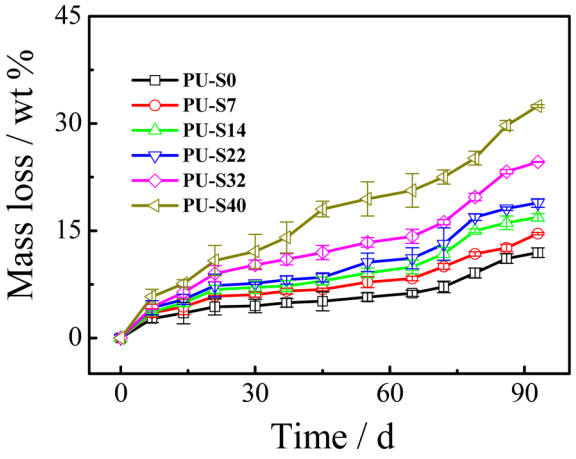

Figure 3. Time dependence of the mass loss of polyurethanes with different PTIPSA contents in ASW at 25 °C.

After immersion in ASW for 7 days, all of the PU-S*x* films start to lose weight. In comparison with PU-S0, polyurethane with PTIPSA side chains generally loses weight faster, indicating a quicker hydrolytic degradation. Moreover, the hydrolytic degradation increases with the PTIPSA content. For PU-S0, the mass loss can be attributed to hydrolysis of the ester linkage in PCL segments.[24,37] In other words, the PCL main chain of polyurethane can also hydrolytically degrade in seawater. For PU-S*x*, the PCL content decreases from 56.4 to 37.3 wt % (Figure S4 in the SI); however, polyurethane with higher PTIPSA content exhibits a higher mass loss. Clearly, hydrolysis of the silyl ester group contributes to degradation more than that of the PCL segments. Actually, hydrolysis of PCL and PTIPSA was studied separately before.[22,37] Indeed, the former hydrolyzes slower than the latter because silyl ester groups are susceptible to hydrolysis because of the larger polarity of the Si−O bond. We evaluated the self-polishing rate in terms of the mass loss per day. It ranges from ∼0.1 to 0.35 wt %/day (see Figure S5 in the SI). Moreover, it increases with the PTIPSA content. Thus, we can design a surface with a controlled self-polishing rate by adjusting the content of PTIPSA side chains.

Figure 4 shows the time dependence of the CA on the surfaces of polyurethanes with different PTIPSA contents.

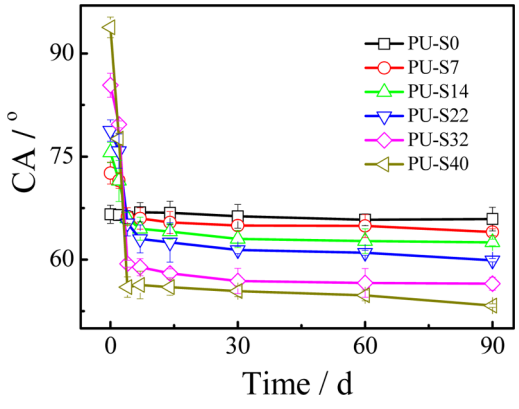

Figure 4. Time dependence of the CA for polyurethanes with different PTIPSA contents in ASW at 25 °C.

Before immersion into ASW, the CAs on the surface of PU-S*x* are larger than that of the PU-S0 surface because the former have hydrophobic triisopropylsilyl ester groups.[43] Moreover, as the PTIPSA content increases, the CA gradually increases, indicating that the hydrophobic PTIPSA moieties covered on the surface increase. After immersion in ASW, the CA for PU-S0 slightly varies. However, the CA for polyurethane with PTIPSA side chains gradually decreases and finally levels off after 7 days. Moreover, as the PTIPSA content increases, the final CA decreases. As reported before,[44,45] hydrolysis of the PCL in PU-S0 can produce carboxyl or alcohol end groups, which has a slight effect on the surface hydrophilicity, so the CA slightly varies. For other PU-S*x*, the rapid decrease in the CA is because hydrolysis of the triisopropylsilyl ester groups yields anionic carboxylate groups and the surface becomes more hydrophilic. This is confirmed by ATR-FTIR (Figure S6 in the SI). The peak intensity at 883 cm^{-1} due to the stretching vibration of the Si−C bond decreases, and the broad band appears around 3300−3500 cm^{-1} due to the stretching vibration of carboxyls after immersion in ASW for 7 days. Accordingly, the final CA decreases with the PTIPSA content.

Figure 5 shows the surface morphologies of the polyurethane films during degradation observed by SEM. For PU-S0, the surface morphology slightly changes after immersion in ASW for 7 days. Actually, it did not exhibit a significant change even after 90 days because PU-S0 has a slow hydrolysis rate due to the high crystallinity and hydrophobicity of the PCL segments.[46] For PU-S22, the surface became rougher after it was exposed to ASW for 7 days owing to the larger surface erosion due to hydrolysis of the triisopropylsilyl ester groups. Yet, the roughness slightly changes with time, indicating that hydrolysis has a slight effect on the surface morphology. For PU-S40, the roughness of the surface also slightly varies with time after exposure to ASW for 7 days; however, it has a roughness larger than that of PU-S22 probably because it has a larger hydrolytic degradation rate (shown in Figure 3). Anyhow, a slight change in the morphology after hydrolysis further indicates a stable self-polishing rate (see Figure S5 in the SI).

The antibiofouling of polyurethane was examined by a marine field test (Figure 6a). For control panels whose surfaces are constructed of epoxy resin, the surfaces were already seriously fouled after 90 days, indicating a heavy fouling pressure. For the panels coated with PU-S*x*, the number of barnacles grown on the surface dramatically decreases as the PTIPSA content increases, indicating that the antibiofouling ability increases with the PTIPSA content. As reported before, the surface constructed by a biodegradable polymer can be gradually decomposed and eroded under seawater or enzymatic attack in marine environments, which can lead to a self-renewal surface polishing the attached living organisms or inorganics away.[24] The antibiofouling ability of PU-S0 is the result of PCL degradation. However, the enhanced antibiofouling performance for PU-S*x* should arise from hydrolysis of the silyl ester group in the side chain besides degradation of PCL in the main chain. In other words, the combination of degradable PCL and hydrolyzable PTIPSA improves hydrolysis and degradation, leading to the enhancement of antibiofouling.

We also used PU-S40 as a carrier and controlled release system for a relatively environmentally friendly antifoulant (DCOIT). To explore the possibility of applications of polyurethane, we chose PMS42 as the control sample. It is a commercial silyl acrylate copolymer containing a content of silyl ester groups close to that of PU-S40, but it does not have

dx.doi.org/10.1021/am4054578 | ACS Appl. Mater. Interfaces 2014, 6, 4017−4024

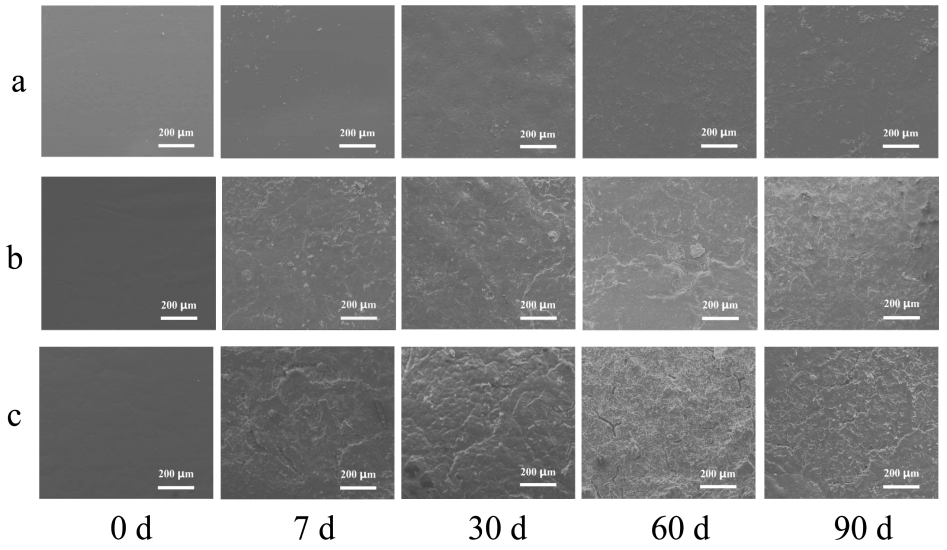

Figure 5. SEM micrographs for the polished surfaces: (a) PU-S0, (b) PU-S22, and (c) PU-S40 after immersion in ASW for different times.

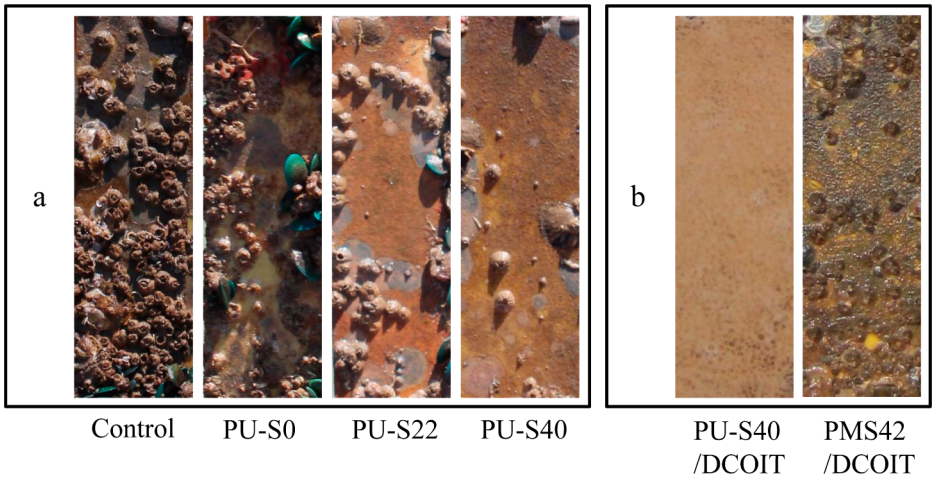

Figure 6. Typical images of tested panels: (a) panels coated with PU-S*x*; (b) panels coated with PU-S40 and PMS-42 in combination with DCOIT (10 wt %) after immersion in seawater for 3 months.

PCL units. Figure 6b shows that the surface constructed by PU-S40 containing DCOIT remains clean within 90 days. However, the surface of the control sample with similar content of silyl ester groups and the same DCOIT is fouled. We also prepared polyurethane with undegradable poly(tetramethylene oxide) segments in the main chain and PTIPSA side chains and tested its antibiofouling property in the absence and presence of DCOIT. As expected, it was also not able to inhibit the settlement of marine organisms (not shown). As we know, the mechanism of self-polishing for a silyl acrylate copolymer involves hydrolysis of the pendant silyl ester groups via seawater attack and dissolution of the resulting hydrolyzed polymer.[17] The balance of hydrolysis and dissolution of the silyl acrylate copolymer is critical. However, dissolution largely depends on shear due to the nonreactive main chain. Thus, the poor antibiofouling ability of the control sample is because it cannot dissolve in a timely manner in static marine environments although it has hydrolyzable PTIPSA moieties, leading to a low release rate of DCOIT. The PU-S*x* with a PCL main chain can degrade in a marine environment because of attack by microorganisms and hydrolysis of the ester linkage, which can significantly improve their dissolution after hydrolysis, leading to enhanced antibiofouling in static marine environments.

CONCLUSION

We have prepared degradable polyurethane with hydrolyzable side chains by the combination of free-radical polymerization and a condensation reaction. Our studies show that polyurethane can enzymatically and hydrolytically degrade in ASW. As the PTIPSA content increases, the hydrolysis rate increases. Marine field tests reveal that polyurethane exhibits enhanced antifouling ability. Polyurethane containing PCL can be used as a carrier and a controlled release system for a relatively environmentally friendly antifoulant. The combination of such a degradable polymer and antifoulant exhibits excellent antibiofouling ability and the promise to hold long-term antifouling performance even in static marine environments.

ASSOCIATED CONTENT

Supporting Information

^{1}H NMR and FTIR spectra on the synthesis of PU-S*x*, DSC and TGA curves of PU-S*x*, and time dependence of the mass

loss rate and ATR-FTIR spectra for PU-S*x*. This material is available free of charge via the Internet at http://pubs.acs.org.

AUTHOR INFORMATION

Corresponding Authors

*E-mail: msmcf@scut.edu.cn.

*E-mail: msgzzhang@scut.edu.cn.

Notes

The authors declare no competing financial interest.

ACKNOWLEDGMENTS

Financial support of the Ministry of Science and Technology of China (Grant 2012CB933802), National Natural Science Foundation of China (Grants 21234003 and 51303059), Science and Technology on Marine Corrosion and Protection Laboratory Open Research Fund (Grant KF120405), and Fundamental Research Funds for Central Universities is acknowledged.

REFERENCES

(1) Yebra, D. M.; Kiil, S.; Dam-Johansen, K. Antifouling Technology-Past, Present and Future Steps Towards Efficient and Environmentally Friendly Antifouling Coatings. *Prog. Org. Coat.* **2004**, *50*, 75−104.

(2) Schultz, M. P.; Bendick, J. A.; Holm, E. R.; Hertel, W. M. Economic Impact of Biofouling on a Naval Surface Ship. *Biofouling* **2011**, *27*, 87−98.

(3) Callow, J. A.; Callow, M. E. Trends in the Development of Environmentally Friendly Fouling-Resistant Marine Coatings. *Nat. Commun.* **2011**, *2*, 244−254.

(4) Finnie, A.; Williams, D. N. In *Paint and Coatings Technology for the Control of Marine Fouling in Biofouling*; Durr, S.; Thomason, J. C., Eds.; Wiley-Blackwell: Chichester, U.K., 2010; p 429.

(5) Thomas, K. V.; Brooks, S. The Environmental Fate and Effects of Antifouling Paint Biocides. *Biofouling* **2010**, *26*, 73−88.

(6) Lejars, M.; Margaillan, A.; Bressy, C. Fouling Release Coatings: A Nontoxic Alternative to Biocidal Antifouling Coatings. *Chem. Rev.* **2012**, *112*, 4347−4390.

(7) Beigbeder, A.; Degee, P.; Conlan, S. L.; Mutton, R. J.; Clare, A. S.; Pettitt, M. E.; Callow, M. E.; Callow, J. A.; Dubois, P. Preparation and Characterisation of Silicone-Based Coatings Filled with Carbon Nanotubes and Natural Sepiolite and Their Application as Marine Fouling-Release Coatings. *Biofouling* **2008**, *24*, 291−302.

(8) Gudipati, C. S.; Greenleaf, C. M.; Johnson, J. A.; Pryoncpan, P.; Wooley, K. L. Hyperbranched Fluoropolymer and Linear Poly-(ethylene glycol) Based Amphiphilic Crosslinked Networks as Efficient Antifouling Coatings: An Insight into the Surface Compositions, Topographies, and Morphologies. *J. Polym. Sci., Part A: Polym. Chem.* **2004**, *42*, 6193−6208.

(9) Krishnan, S.; Ramakrishnan, A.; Hexemer, A.; Finlay, J. A.; Sohn, K. E.; Perry, R.; Ober, C. K.; Kramer, E. J.; Callow, M. E.; Callow, J. A.; Fischer, D. A. Anti-Biofouling Properties of Comblike Block Copolymers with Amphiphilic Side Chains. *Langmuir* **2006**, *22*, 5075−5086.

(10) Wang, Y. P.; Finlay, J. A.; Betts, D. E.; Merkel, T. J.; Luft, J. C.; Callow, M. E.; Callow, J. A.; DeSimone, J. M. Amphiphilic Co-Networks with Moisture-Induced Surface Segregation for High-Performance Nonfouling Coatings. *Langmuir* **2011**, *27*, 10365−10369.

(11) Wang, Y. P; Betts, D. E.; Finlay, J. A.; Lenora, H. B.; Callow, M. E.; Callow, J. A.; Wendt, D. E.; DeSimone, J. M. Photocurable Amphiphilic Perfluoropolyether/Poly(ethylene glycol) Networks for Fouling-Release Coatings. *Macromolecules* **2011**, *44*, 878−885.

(12) Wang, Y. P.; Pitet, L. M.; Finlay, J. A.; Lenora, H. B.; Cone, G.; Betts, D. E.; Callow, M. E.; Callow, J. A.; Wendt, D. E.; Hillmyer, M. A.; DeSimone, J. M. Investigation of the Role of Hydrophilic Chain Length in Amphiphilic Perfluoropolyether/Poly(ethylene glycol) Networks: Towards High-Performance Antifouling Coatings. *Biofouling* **2011**, *27*, 1139−1150.

(13) Zhang, Z.; Finlay, J. A.; Wang, L.; Gao, Y.; Callow, J. A.; Callow, M. E.; Jiang, S. Y. Polysulfobetaine-Grafted Surfaces as Environmentally Benign Ultralow Fouling Marine Coatings. *Langmuir* **2009**, *25*, 13516−13521.

(14) Jiang, S. Y.; Cao, Z. Ultralow-Fouling, Functionalizable, and Hydrolyzable Zwitterionic Materials and Their Derivatives for Biological Applications. *Adv. Mater.* **2010**, *22*, 920−932.

(15) Xie, L. Y.; Hong, F.; He, C. X.; Ma, C. F.; Liu, J. H.; Zhang, G. Z.; Wu, C. Coatings with a Self-Generating Hydrogel Surface for Antifouling. *Polymer* **2011**, *52*, 3738−3744.

(16) Thorlaksen, P.; Yebra, D. M.; Catala, P. Hydrogel-Based Third Generation Fouling Release Coatings. *Gallois Mag.* **2010**, *5*, 218−224.

(17) Bressy, C.; Margaillan, A. Faÿ, F.; Linossier, I.; Vallée-Réhel, K. In *Advances in Marine Antifouling Coatings and Technologies*; Hellio, C., Yebra, D. M., Eds.; Woodhead Publishing: Cambridge, U.K., 2009; p 459.

(18) Almeida, M.; Diamantino, T. C.; de Sousa, O. Marine Paints: The Particular Case of Antifouling Paints. *Prog. Org. Coat.* **2007**, *59*, 2−20.

(19) Fukuda, S.; Honda, Y.; Itoh, M.; Masuoka, S.; Taniguchi, M. Metal-Free Binders for Self-Polishing Antifouling Paints. U.S. Patent 5,436,284, 1995.

(20) Oya. M.; Nakamura, N.; Tsuboi, M. Antifouling Coating Composition, Coating Film Therefrom, Base Material Covered with the Coating Film and Antifouling Method. U.S. Patent 6,916,860 B2, 2005.

(21) Longo, F. N.; Gardega, T. Polymer Based Antifouling Coating. U.S. Patent219944 A1, 2008.

(22) Bressy, C.; NGuyen, M. N.; Tanguy, B.; Ngo, V. G.; Margaillan, A. Poly(trialkylsilyl methacrylate)s: A Family of Hydrolysable Polymers with Tuneable Erosion Profiles. *Polym. Degrad. Stab.* **2010**, *95*, 1260−1268.

(23) Bressy, C.; Hellio, C.; NGuyen, M. N.; Tanguy, B.; Maréchal, J.-P.; Margaillan, A. Optimized Silyl Ester Diblock Methacrylic Copolymers: A New Class of Binders for Chemically Active Antifouling Coatings. *Prog. Org. Coat.* **2014**, *77*, 665−673.

(24) Ma, C. F.; Xu, L. G.; Xu, W. T.; Zhang, G. Z. Degradable Polyurethane for Marine Anti-Biofouling. *J. Mater. Chem. B* **2013**, *1*, 3099−3106.

(25) Liu, G. B.; Zhao, H. Y.; Thiemann, T. Triphenylphosphine-Catalyzed Dehydrogenative Coupling Reaction of Carboxylic Acids with Silanes—A Convenient Method for the Preparation of Silyl Esters. *Adv. Synth. Catal.* **2007**, *6*, 807−811.

(26) Liu, G. B. Preparation of Silyl Esters by $ZnCl_2$-Catalyzed Dehydrogenative Cross-Coupling of Carboxylic Acids and Silanes. *Synlett* **2006**, *9*, 1431−1433.

(27) Ma, C. F.; Zhou, H.; Wu, B.; Zhang, G. Z. Preparation of Polyurethane with Zwitterionic Side Chains and Their Protein Resistance. *ACS Appl. Mater. Interfaces* **2011**, *3*, 455−461.

(28) Ma, C. F.; Bi, X. B; Ngai, T.; Zhang, G. Z. Polyurethane-Based Nanoparticles as Stabilizers for Oil-in-Water or Water-in-Oil Pickering Emulsions. *J. Mater. Chem. A* **2013**, *1*, 5353−5360.

(29) Ding, M. M.; Li, J. H.; Fu, X. T.; Zhou, J.; Tan, H.; Gu, Q.; Fu, Q. Synthesis, Degradation, and Cytotoxicity of Multiblock Poly(ε-caprolactone urethane)s Containing Gemini Quaternary Ammonium Cationic Groups. *Biomacromolecules* **2009**, *10*, 2857−2865.

(30) Han, J.; Chen, B.; Ye, L.; Zhang, A. Y.; Zhang, J.; Feng, Z. G. Synthesis and Characterization of Biodegradable Polyurethane Based on Poly(ε-caprolactone) and L-Lysine Ethyl Ester Diisocyanate. *Front. Mater. Sci. China.* **2009**, *3*, 25−32.

(31) Sivakumar, C.; Nasar, A. S. Poly(ε-caprolactone)-Based Hyperbranched Polyurethanes Prepared via A2+B3 Approach and Its Shape-Memory Behavior. *Eur. Polym. J.* **2009**, *45*, 2329−2337.

(32) Sauerbrey, G. Use of Quartz Vibration for Weighing Thin Films on a Microbalance. *Z. Phys.* **1959**, *155*, 206−212.

(33) Voinova, M. V.; Rodahl, M.; Jonson, M.; Kasemo, B. Viscoelastic Acoustic Response of Layered Polymer Films at Fluid−Solid Interfaces: Continuum Mechanics Approach. *Phys. Scr.* **1999**, *59*, 391−396.

(34) Liang, H. M.; Miranto, H.; Granqvist, N.; Sadowski, J. W.; Viitala, T.; Wang, B. C.; Yliperttula, M. Surface Plasmon Resonance Instrument as a Refractometer for Liquids and Ultrathin Films. *Sens. Actuators, B* **2010**, *149*, 212−220.
(35) Liu, J. T.; Chen, C. J.; Ikoma, T.; Yoshioka, T.; Cross, J. S.; Chang, S. J.; Tsai, J. Z.; Tanaka, J. Surface Plasmon Resonance Biosensor with High Anti-Fouling Ability for the Detection of Cardiac Marker Troponin T. *Anal. Chim. Acta* **2011**, *703*, 80−86.
(36) Yu, J. Biodegradation-Based Polymer Surface Erosion and Surface Renewal for Foul-Release at Low Ship Speeds. *Biofouling* **2003**, *19*, 83−90.
(37) Rutkowska, M.; Krasowska, K.; Heimowska, A.; Steinka, I.; Janik, H.; Haponiuk, J.; Karlsson, S. Biodegradation of Modified Poly(ε-caprolactone) in Different Environments. *Pol. J. Environ. Stud.* **2002**, *4*, 413−420.
(38) Hou, Y.; Chen, J.; Sun, P. J.; Gan, Z. H.; Zhang, G. Z. In Situ Investigations on Enzymatic Degradation of Poly(ε-caprolactone). *Polymer* **2007**, *48*, 6348−6353.
(39) Rodahl, M.; Höök, F.; Krozer, A.; Kasemo, B.; Breszinsky, P. Quartz Crystal Microbalance Setup for Frequency and Q-factor Measurements in Gaseous and Liquid Environments. *Rev. Sci. Instrum.* **1995**, *66*, 3924−3930.
(40) Dovrzynski, P.; Li, S.; Kasperczyk, J.; Bero, M.; Gasc, F.; Vert, M. Structure−Property Relationships of Copolymers Obtained by Ring-Opening Polymerization of Glycolide and ε-Caprolactone. Part 1. Synthesis and Characterization. *Biomacromolecules* **2005**, *6*, 483−488.
(41) Gu, X. Z.; Wu, J.; Mather, P. T. Polyhedral Oligomeric Silsesquioxane (POSS) Suppresses Enzymatic Degradation of PCL-Based Polyurethanes. *Biomacromolecules* **2011**, *12*, 3066−3077.
(42) Vogt, B. D.; Eric, K. L.; Wu, W. L.; Christopher, C. W. Effect of Film Thickness on the Validity of the Sauerbrey Equation for Hydrated Polyelectrolyte Films. *J. Phys. Chem. B* **2004**, *108*, 12685−12690.
(43) Hong, F.; Xie, L. Y.; He, C. X.; Liu, J. H.; Zhang, G. Z.; Wu, C. Effects of Hydrolyzable Comonomer and Cross-linking on Anti-Biofouling Terpolymer Coatings. *Polymer* **2013**, *54*, 2966−2972.
(44) Faÿ, F.; Renard, E.; Langlois, V.; Linossier, I.; Vallée-Réhel, K. Development of Poly(ε-caprolactone-*co*-L-lactide) and Poly(ε-caprolactone-*co*-δ-valerolactone) as New Degradable Binder Used for Antifouling Paint. *Eur. Polym. J.* **2007**, *43*, 4800−4813.
(45) Bellenger, V.; Ganem, M.; Mortaigne, B.; Verdu, J. Lifetime Prediction in the Hydrolytic Ageing of Polyesters. *Polym. Degrad. Stab.* **1995**, *49*, 91−97.
(46) Báez, J. E.; Ramírez, D.; Valentín, J. L.; Marcos-Fernández, A. Biodegradable Poly(ester-urethane-amide)s Based on Poly(ε-caprolactone) and Diamide-Diol Chain Extenders with Crystalline Hard Segments. Synthesis and Characterization. *Macromolecules* **2012**, *45*, 6966−6980.